2.0 ANALYTICAL MODELS OF THERMAL EXCHANGES IN THE PYRANOMETER

In Chapter 1, it was established that a better understanding of the thermal exchanges within the instrument is necessary to define the quantities producing an offset. In this chapter, we review several radiative studies of the pyranometer and a similar radiometer, the pyrgeometer. The conclusion of this chapter is a correction model for the instrument measurements.

2.1 Pyrgeometer Models

Several analytical models have been developed for the pyranometer's sister instrument, the pyrgeometer. In 1970, Drummond et al. described the development of an instrument designed to directly measure longwave radiative fluxes. Use of this pyrgeometer replaced the procedure of determining longwave fluxes by subtracting the measured shortwave from net fluxes [Albrect and Cox, 1977]. The Eppley Precision Infrared Radiometer (PIR) model pyrgeometer uses the same thermopile principles of operation as the pyranometer to measure incident longwave radiation (4-50 μm). The sensor of the PIR is shielded by a filter that limits the responsivity of the instrument to the thermal spectrum. It has been shown that the KRS-5 dome with an interference filter designed to transmit thermal radiation will absorb and reflect solar radiation in the visible spectrum [Duchon and Wilk, 1994]. This creates a temperature differential between the dome and the sensor. As in the case of the PSP, thermal radiation emitted from the interior of the dome adds to that transmitted through the dome, offsetting the true measurement signal. For several years, various groups have attempted to quantify this varying offset due to solar heating and thermal radiative cooling in order to develop an analytical correction for the pyrgeometer signal.

In 1977, Albrecht and Cox developed a procedure to improve measurements of the pyrgeometer by considering the thermal exchanges within the instrument. An analytical expression for a budget of energy within the instrument revealed that the actual flux being measured from a signal output could be represented by

$$F = U_{emf}\left(c_1 + c_2 T_s^3\right) + \varepsilon_0 \sigma T_s^4 - k\sigma\left(T_d^4 - T_s^4\right), \qquad (2.1)$$

where F = incident irradiance to the instrument (W/m^2),

U_{emf} = thermopile signal (V),

T_s = temperature of sensor (K),

T_d = temperature of KRS-5 filter (K),

ε_o = effective emissivity of the sensor surface,

and σ = Stefan-Boltzmann constant = 5.67 x 10^{-8} W/m^2K^4.

The manufacturer's calibration of the pyrgeometer determines the constants of k, c_1 and c_2. Internal circuitry is designed to compensate for the T_s^3 and T_s^4 term. The (T_d^4-T_s^4) term does not come into play because the dome and sensor are maintained at the same temperature during calibration. During operation, however, the solar heating typically produces as much as a 10°C difference between the filter dome and the instrument body temperature. Using their analysis, Albrecht and Cox determine that a 0.1°C uncertainty between dome and heat sink temperatures may result in a 3 to 4 W/m^2 error in measurement, which makes the solar heating effect significant. They propose modifying the instrument to monitor of the sink and dome temperature as a function of time, and then to use that information with the thermopile output to increase the accuracy of the data.

Philipona et al. [1995] propose a modification to the pyrgeometer that provides the temperature information needed to account for thermal fluxes within the dome. A similar energy balance was performed within the KRS-5 dome. The Albrecht and Cox equation, Equation 2.1, was modified slightly to include higher-order terms and previously determined instrument quantities. The proposed correction to be applied to the pyrgeometer signal is

$$E_L = \frac{U_{emf}}{c}\left(1 + k_1\sigma T_B^3\right) + k_2\sigma T_B^4 - k_3\sigma\left(T_D^4 - T_B^4\right), \qquad (2.2)$$

where c = sensitivity of the pyrgeometer (V / Wm^{-2}), and

k_1, k_2 and k_3 are parameters that may be derived from the optical properties of the dome and sensor and the operational characteristics of the thermopile.

The analysis by Philipona et al. does not treat multiple reflections within the KRS-5 dome. In fact, multiple reflections of thermal radiation are not much of an issue in the pyrgeometer since the filters are designed to transmit this radiation. That is, thermal radiation leaving the sensor surface, or other internal surfaces, is much more likely to pass through the filter dome out of the instrument than to be reflected back on the sensor and interfere with the

signal. In the pyranometer, however, the filters are designed to absorb or reflect thermal radiation so that multiple reflections among the internal surfaces must be considered.

Philipona et al. propose to modify the pyrgeometer by adding three thermistors to the inside surface of the dome at a 45-deg angle from the base and spaced 120-deg from each other. The average of these three thermistors would represent any axial variation in dome temperature. The 45-deg location was hypothesized to represent variations in dome temperature along the dome zenith.

2.2 The Bush Model

Algorithms to correct for the zero offset in the pyranometer have been developed using experimental results. In 1998, Bush et al. described an effort to correct pyranometer measurements using an empirical model to account for thermal exchanges between the dome and the sensor. The result of this model is a linear approximation to the difference of the temperatures to the fourth power. The correction to be applied in this model is expressed as the offset quantity

$$\Delta F = 4.0537 \times 10^{-8} (T_{Dome}^4 - T_{Detector}^4) - 0.0828 \quad [\mathrm{W/m^2}]. \tag{2.3}$$

The coefficients in Equation 2.3 apply to the instrument used in the experiment. These would be determined for an individual instrument in calibration. In operation, this correction requires that the temperatures of the dome and sensor be continuously monitored to correct data for a corresponding period of time. Bush et al. proposed a modification to the pyranometer that employed four thermistors. Two thermistors are mounted under the instrument floor near the sensor and two are attached to the outer dome. The dual thermistors sample spatial variations in temperature. This model is strictly empirical and does not involve the physical processes of energy exchange within the instrument. Specifically, it neglects the additional exchanges within the instrument due to reflections and wavelength-dependant surface properties in favor of a linear approximation.

The effect of these strategic modifications on the performance of the pyranometer must also be a source of concern. The temperature of the sensor cannot be directly measured without altering its temperature, thereby affecting the measurement. Therefore, the team decided to compromise and placed the thermistors near the sensor rather than directly on the sensor to obtain an approximation to its temperature. The heads of the thermistors mounted on the dome

were shielded from direct sunlight so that they would not absorb solar radiation. However, this shielding, as well as the thermistors and leads will block some solar radiation from reaching the sensor. The shielding will also reduce the local temperature on the dome itself.

2.3 The Haeffelin Model

In a 1999 paper, Haeffelin et al. propose a correction for the pyranometer similar to that embodied in the Philipona model of the pyrgeometer. They conclude that the instrument measurement may be corrected to the desired shortwave irradiance, E, by

$$E = U_{emf}\left[\frac{1}{\alpha_s \tau_d c} + \frac{4\sigma}{S\tau_d}(1-\varepsilon_s \rho_d)T_b^3\right] + \frac{\varepsilon_d \sigma}{\tau_d}(\varepsilon_s T_b^4 - T_d^4) + \frac{\sigma}{\tau_d}(1-\alpha_s)T_b^4. \qquad (2.4)$$

The physics behind the correction embodied in Equation 2.4 are described in detail in Section 2.4.

2.4 Physics within the Haeffelin Model

An analysis similar to that of Philipona et al. describes the physical processes involved in the thermal offset. Reasonable assumptions are used to arrive at Haeffelin's correction expression, Equation 2.4. The origins of the net radiative flux arriving at the sensor surface are determined using the radiation model shown in Figure 2.1. Three sources of radiation are considered. The incident solar flux on the instrument arrives after being transmitted through the filter. Thermal radiation emitted from the dome arrives at the sensor surface. In addition, thermal radiation emitted by the sensor surface is reflected back to the sensor by the dome, which does not allow thermal radiation to transmit. This latter radiation either returns to the sensor surface, or is absorbed by the dome, thereby contributing to the dome heating.

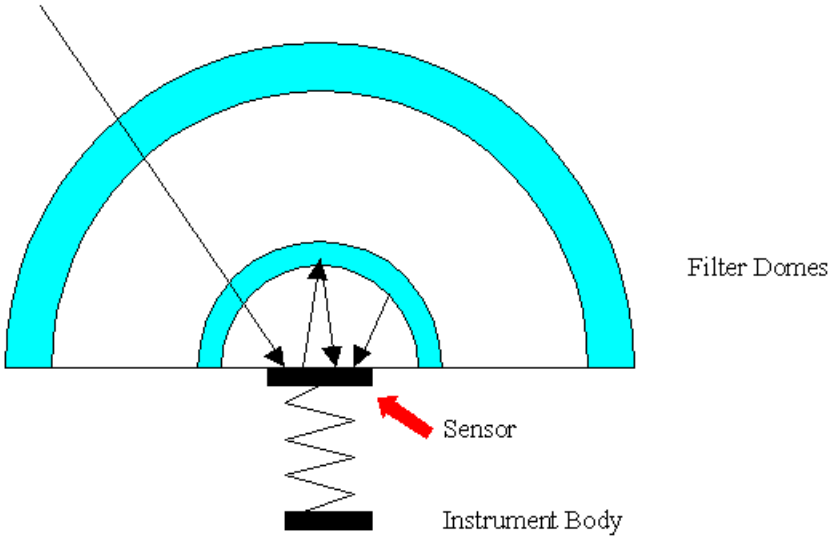

Figure 2.1 Radiative heat transfer in pyranometer analytical model

Though the shortwave and longwave components of flux arriving at the sensor surface may be found separately, the sensor measures total net flux. The optical properties of the lacquer are essentially black for all wavelengths, so that the longwave (^{L}) and shortwave (^{S}) properties are the same. This leads to the relations

$$F_{net}^{S} = E^{S}\tau_{d}^{S}\alpha_{s}^{S}\,, \tag{2.5}$$

$$F_{net}^{L} = E^{L}\tau_{d}^{L}\alpha_{s}^{L} + \sigma T_{d}^{4}(\phi)\varepsilon_{d}^{L}\alpha_{s}^{L} + \sigma T_{s}^{4}\varepsilon_{s}^{L}\rho_{d}^{L}\alpha_{s}^{L} - \sigma T_{s}^{4}\varepsilon_{s}^{L}\,, \tag{2.6}$$

and

$$F_{net} = \alpha_{s}\tau_{d}E + \alpha_{s}\varepsilon_{d}\sigma T_{d}^{4} + \alpha_{s}\varepsilon_{s}\rho_{d}\sigma T_{s}^{4} - \varepsilon_{s}\sigma T_{s}^{4}\,; \tag{2.7}$$

where E = external irradiance (W/m^2), longwave irradiance is blocked by domes, and

T_d = inner dome temperature, it is assumed a representative dome temperature can simulate the flux condition of the dome gradient, $T_d(\phi)$.

The signal produced by the thermopile is assumed to be a linear function of the difference in temperature between the sensor surface and the instrument body temperature when operating under normal conditions. The signal may be converted to an irradiance measurement using the sensitivity relation

$$U_{emf} = S(T_s - T_b) = c(F_{net}), \tag{2.8}$$

where U_{emf} is the voltage signal (μV),

S is the thermopile Seebeck coefficient (μV/K),

T_s and T_b are the sensor and body temperature, respectively (K),

and c is the instrument sensitivity (V / Wm^{-2}).

Using these assumptions, the temperature of the sensor and the net flux arriving at the sensor surface are derived from measurable quantities; that is

$$T_s = T_b + \frac{U_{emf}}{S} \tag{2.9}$$

and

$$F_{net} = \frac{U_{emf}}{c}. \tag{2.10}$$

Equation 2.7 is solved for the quantity of interest, E, which results in Equation 2.7a. The unknown quantities, F_{net} and T_s, are replaced with measurable quantities, T_b and U_{emf} in Equation 2.7b. The last two terms of Equation 2.7b are then expanded. The quantity T_b is on the order of 300 K and U_{emf}/S is typically less than 3 K. The third term of the expansion is less than 0.06 percent of the first, so the first two terms of the expansion are sufficient to approximate the expansion. Under this approximation, Equation 2.7 becomes

$$E = \frac{F_{net}}{\alpha_s \tau_d} - \frac{\varepsilon_d \sigma T_d^{\,4}}{\tau_d} - \frac{\varepsilon_s \rho_d \sigma T_s^{\,4}}{\tau_d} + \frac{\varepsilon_s \sigma T_s^{\,4}}{\alpha_s \tau_d}, \tag{2.7a}$$

or

$$E = \frac{U_{emf}}{c\alpha_s \tau_d} - \frac{\varepsilon_d \sigma T_d^{\,4}}{\tau_d} - \frac{\varepsilon_s \rho_d \sigma \left(T_b + \frac{U_{emf}}{S}\right)^4}{\tau_d} + \frac{\varepsilon_s \sigma \left(T_b + \frac{U_{emf}}{S}\right)^4}{\alpha_s \tau_d}, \tag{2.7b}$$

or finally,

$$E = U_{emf}\left(\frac{1}{c\alpha_s \tau_d} + \frac{4\varepsilon_s \sigma (1 - \alpha_s \rho_d)}{S\alpha_s \tau_d} T_b^3\right) + \frac{\varepsilon_s \sigma (1 - \alpha_s \rho_d)}{\alpha_s \tau_d} T_b^{\,4} - \frac{\varepsilon_d \sigma}{\tau_d} T_d^{\,4}. \tag{2.7c}$$

With the inclusion of the greybody assumption ($\alpha_s = \varepsilon_s$), Equation 2.7c becomes Equation 2.4.

2.5 Model Implications

The analytical formulation of the thermal exchanges within the pyranometer offers insight into the information needed to correct measurements. Equation 2.7c suggests that an

instrument may be calibrated to account for thermal effects when the inner dome temperature and the instrument body temperature are monitored.

Because of its large thermal mass, the instrument body temperature is assumed to be uniform throughout, and changing only slowly. Therefore, its temperature measurement location is not critical, but it should be taken as close to the cold junction of the thermopile as possible to avoid including any gradients that may be present in the body.

Monitoring the dome temperature does pose problems. First, the dome does not have a single uniform temperature. Rather, a temperature distribution is present that varies from the instrument body temperature at the base of the glass to an extreme temperature at the vertex of the dome, or near the vertex if the dome is exposed to a non-uniform environment. It is hypothesized that a single temperature can represent the distribution in Equation 2.7c. Then the net irradiance arriving at the surface of the sensor from a thermally uniform dome at this temperature is the same as that arriving from the dome with a gradient of temperature. A location for measuring this temperature is determined by examining temperature distributions that exist under various conditions, and then identifying a representative temperature on the distribution.

Another concern in measuring the dome temperature is a transient effect. The domes have a small thermal mass, and their temperatures may vary or fluctuate quickly. The possibility exists that the thermopile measuring a temperature may not record the thermal history with much precision because the thermopile itself has thermal mass and its leads may conduct heat to or from the attachment point to the dome.

A finite element model of the pyranometer is helpful in determining an appropriate location for the dome temperature measurement. Representing the physical system numerically will provide a detailed description of the dome temperature gradient, which may be interpreted as described above to determine an ideal location to monitor the representative dome temperature. Chapter 3 describes the construction of a numerical model of the pyranometer domes. This model is used to determine the ideal location to measure the representative temperature under various conditions.